Bioelectrochemistry 136 (2020) 107595

Contents lists available at ScienceDirect

Bioelectrochemistry

journal homepage: www.elsevier.com/locate/bioelechem

A low fouling electrochemical biosensor based on the zwitterionic polypeptide doped conducting polymer PEDOT for breast cancer marker BRCA1 detection

Jiasheng Wang [1], Dongwei Wang [1], Ni Hui *

Qingdao Agricultural University, Qingdao 266109, China

ARTICLE INFO

Article history:
Received 22 December 2019
Received in revised form 2 July 2020
Accepted 2 July 2020
Available online 13 July 2020

Keywords:
Antifouling biosensor
Polypeptide
Conducting polymer
PEDOT
DNA sensor

ABSTRACT

The application of polypeptides in bio-interfaces and biosensors is of great interest because polypeptides are biocompatible and easy to design. A novel polymer nanocomposite was prepared by the electropolymerization of the conducting polymer poly(3,4-ethylenedioxythiophene) (PEDOT) with a newly designed polypeptide. The nanocomposite polypeptide doped PEDOT (PEDOT/PEP), with a 3D microporous network structure, large surface area and excellent antifouling ability, was utilized for the attachment of BRCA1 complementary oligonucleotides to construct a DNA biosensor. The fabricated DNA biosensor showed favorable selectivity (with a detection limit of 0.0034 pM) and high sensitivity. The biosensor was also capable of detecting the target DNA (BRCA1) in 1% (V/V) human serum samples. The combination of a conducting polymer PEDOT with an antifouling and biocompatible polypeptide demonstrates a new method for preparing electrochemical sensors, that are capable of detecting targets in complex biological samples without strong nonspecific protein adsorption.

1. Introduction

Biosensors have attracted much attention since their invention for applications in clinical disease diagnosis, food detection and environmental supervision [1–3]. Electrochemical biosensors are low cost and simple to operate and have become important in supporting high levels of assay sensitivity [4,5]. Real clinical applications of electrochemical biosensors can be challenging because nonspecific adsorption of proteins in serum samples or other complex media can produce large background signal and limit accuracy and precision. An effective way to resolve this issue is to integrate recognition into the sensing surface that is highly antifouling [6]. Previous studies have demonstrated that various low-fouling functional materials are highly hydrophilic and/or zwitterionic, such as poly(ethylene glycol) (PEG), oligo(ethylene glycol) (OEG), and nonionic or zwitterionic polymers [6–9]. PEG and OEG motifs have been the most widely utilized antifouling polymers but they are subject to oxidation in the presence of transition-metal ions and oxygen, both of which are present in most biochemically relevant conditions [10]. Zwitterionic polymers, such as poly(carboxybetaine) and poly(sulfobetaine) have good antifouling performance even in real media due to their strong hydration capacity via electrostatic interactions [11,12]. Jiang et al. reported that phosphorylcholine self-assembled monolayers have strong resistance to protein adsorption. Both experimental and molecular simulation techniques have proved that having balanced charge and minimized dipole are two key factors for their antifouling behavior [13]. However, the time-consuming and complex synthesis procedure seriously restrict their application.

An ideal antifouling interface should have the following characteristics: high antifouling property, good biocompatibility, convenient electrode integration and being easily modifiable with biomolecules [14–16]. Polypeptides with specific sequences are new group of antifouling materials that have been attracting attention recently [17]. Polypeptides are composed of natural amino acids, which have naturally superior biocompatibility and exist as zwitterionic molecules in biological systems [18]. Recent studies have shown that a series of polypeptides have antifouling property. For example, Jiang's group has reported that the inclusion of an additional linker of four residues in length (-PPPPC) of a rigid, hydrophobic nature, is a better choice for forming peptide self-assembled monolayers with well-ordered structures. The experimental results proved that EKEKEKE-PPPPC-Am forms a secondary structure and shows excellent antifouling ability for fibrinogen and lysozyme [19]. Su's group synthesized a zwitterionic polypeptide (CREREREE) that demonstrated relatively high antifouling property in single pro-

* Corresponding author.
E-mail address: huini1029@163.com (N. Hui).
[1] These authors contributed equally to this work.

https://doi.org/10.1016/j.bioelechem.2020.107595
1567-5394/

tein and real media, compared to an amphiphilic, non-ionic polypeptide (CYSYSYS) [17]. The molecular structures of the amphiphilic peptide and the zwitterionic peptide are shown in Fig. S1 of the supporting materials. Following the general design principles for producing antifouling materials with excellent hydrophilicity and electrical neutrality [20], we designed a polypeptide sequence (CPPPPNQNQNQNQ) that has been used to construct a sensing surface to explore the protein-resistance ability in this work.

It should be noted that polypeptides, which are not conductive, can increase the impedance of the electrode and decrease its sensitivity. It is expected that the combination of polypeptides with conducting polymers, may contribute to a solution to this problem. Recently, conducting polymers, like polyaniline, polypyrrole, and polythiophene, have emerged as promising materials in a variety of applications such as biosensors, antistatic coatings, supercapacitors, chemical sensors, electronic devices, light emitting diodes, and batteries [21–24]. Amongst these polymers, poly(3,4-ethylene dioxythiophene) (PEDOT) is considered one of the most stable and successful commercially available conducting polymers. PEDOT has drawn considerable attention for the development of chemo/biosensors because of its high conductivity, great environmental stability, biocompatibility, low toxicity, and well-defined chemical structure [25–27]. For instance, PEDOT composite modified electrodes have been successfully used for the detection of heavy metals such as Hg, Cd, Pb, Cu and metalloid As. As an adsorbent in the preconcentration process, PEDOT-based materials can synergistically enhance the conductivity and stability of composites that play an important role in the adsorption and enrichment of heavy metals [28,29]. PEDOT-based materials have been widely utilized for the sensitive and selective determination of carcinoembryonic antigens, alpha fetoproteins, the influenza A virus, C-reactive proteins, DNA sequences and glucose due to the electrostatic properties, biocompatibility and easy immobilization of biomolecule [14,30–32]. However, due to high background signal and delayed responses produced by nonspecific protein adsorption, performing assays in complex media using PEDOT sensors has been challenging.

The breast cancer susceptibility gene (BRCA1) is an important tumour marker for breast cancer, ovarian cancer, pancreatic cancer and colon cancer [33]. Medical science has now proven that BRCA1 plays an important role in several cellular pathways that support genomic stability, such as DNA mending, protein ubiquitination, chromatin remodeling, and apoptosis [34]. Therefore, the reliable detection of BRCA1 at low concentrations is important for multiple research fields including diagnostics and forensics. In this work, an electrochemical DNA biosensor was developed for quantitative analysis of BRCA1 in complex samples. First, a novel conducting polymer nanocomposite of PEDOT doped with a polypeptide sequence was prepared through a simple electrodeposition method. The nanocomposite integrated the suitable compatibility, excellent conductivity, and stability of PEDOT with the strong antifouling ability and biocompatibility of the polypeptide, which results in an ideal substrate for a biosensor. The polypeptide used in this study can act as a bifunctional material that not only inhibits the nonspecific adsorption of proteins but also allows for the usage of its carboxylic to fix DNA probes (terminated with amino group), as shown in Scheme 1. The proposed PEDOT/PEP-based biosensor showed good analytical performance (ultrahigh sensitivity, low detection limit and antifouling ability) and proved to be capable of successfully detecting BRCA1 even in 1% (V/V) human serum samples.

2. Materials and methods

2.1. Regents

3,4-Ethylenedioxythiophene (EDOT), $LiClO_4$, methylene blue (MB) 1-ethyl-3-(3-dimethylaminopropyl) carbodiimide (EDC), and N-hydroxysuccinimde (NHS) were purchased from Aladdin Reagents (Shanghai, China). The polypeptides used in this work (CPPPPNQNQNQNQ, purity > 99%) were both synthesized and purified by Bankpeptide biological technology Co. Ltd. (Hefei, China). The structures of the polypeptide sequences are shown in Fig. S1. Bovine serum albumin (BSA), adenosine triphosphate (ATP), carcinoembryonic antigen antibody (CEA), alpha fetoprotein antibody (AFP), lysozyme (LZ), human serum albumin (HSA) and DNA were all obtained from Sangon Biotench. Co., Ltd. (Shanghai, China). The DNA samples were purified by high-performance liquid chromatography (HPLC) and used as received. The capture DNA probe (C1), target DNA (BRCA1) (T2), one-base mismatched DNA (M1), three-base mismatched DNA (M2) and non-complementary DNA (M3) sequences are shown in Table S1. Human serum samples were supplied by Qingdao Chengyang People Hospital.

2.2. Apparatus

All electrochemical experiments were performed using a CHI660E electrochemical station (Shanghai Chenhua Instrument Co., Ltd., China). A three-electrode system was employed with a modified glassy carbon electrode (GCE, diameter 3.0 mm), an Ag/AgCl electrode and a platinum wire. Static water contact angle measurements were performed on JC2000-CG400 goniometer by the sessile drop method (Shanghai Zhongchen Instrument Co., China). The morphologies of PEDOT/PEP and PEDOT/$LiClO_4$ were characterized using field emission scanning electron microscope (SEM) (JEOL JSM-7500F, Hitachi High-Technology Co., Ltd., Japan). X-Ray photoelectron spectroscopy (XPS) analysis was performed using an ESCALAB 250Xi spectrometer (Thermo Fisher Scientific, UK) with a high-performance Al monochromatic source operated at 15 kV.

2.3. Synthesis of PEDOT/PEP onto GCE surface

Following the methods of our previous report, the GCE was polished and pre-treated before use [35]. As shown in Scheme 1, polypeptide doped PEDOT nanocomposites (PEDOT/PEP) were electrodeposited onto the pretreated GCE surface in a solution containing 1 mg mL^{-1} polypeptide and 0.01 M EDOT, using cyclic voltammetry (CV) (parameters: −0.2–1.2 V; scan rate: 0.1 V s^{-1}; 15 cycles). For comparison, $LiClO_4$ doped PEDOT nanocomposites (PEDOT/$LiClO_4$) were also prepared using the same method with a 0.01 M EDOT solution containing 0.094 mM $LiClO_4$ as the electrolyte. GCEs modified with PEDOT/PEP or PEDOT/$LiClO_4$ were defined as GCE/PEDOT/PEP and GCE/PEDOT/$LiClO_4$, respectively.

2.4. Preparation and sensing performance of the DNA biosensor

The fabrication process for the DNA sensor based on PEDOT/PEP is shown in Scheme 1. Phenothiazine dye methylene blue (MB) is one of the most popular redox indicators and MB has shown much higher affinity to ssDNA rather than dsDNA [36]. MB has been widely used as an excellent redox indicator in a variety of electrochemical DNA assays [37]. The electrochemical properties of the electrodes for detecting the signal from MB are highly important for the fabrication of electrochemical DNA biosensors with high performances [37,38]. GCE/PEDOT/PEP was incubated in 1.0 μM capture DNA (C1) solution, which included 0.4 M EDC and 0.1 M NHS, for 2 h to allow GCE/PEDOT/PEP to covalently attach C1. The obtained biosensor was defined as GCE/PEDOT/PEP/C1. To monitor the hybridization reactions and perform electrochemical detection, GCE/PEDOT/PEP/C1 was immersed into 1 mL of MB solution (20 μM) for 60 min to attach MB into the DNA sequence (C1), followed by rinsing with PBS and water three times. This biosensor was defined as GCE/PEDOT/PEP/C1/MB. The hybridization reaction

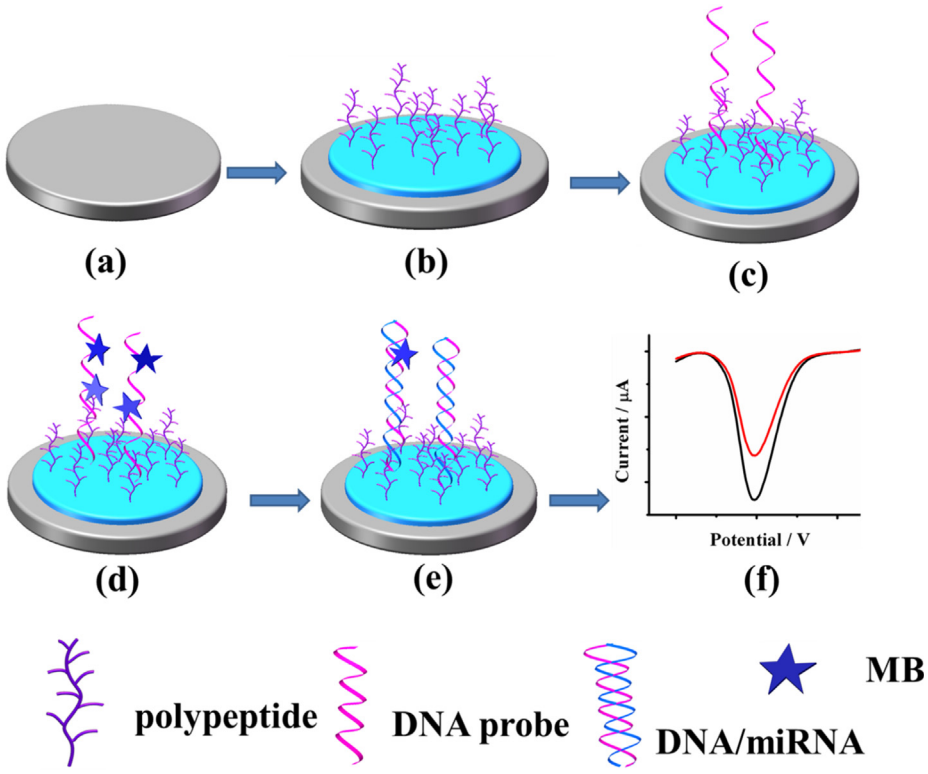

Scheme 1. schematic illustration of the fabrication process of antifouling BRCA1 biosensor based on PEDOT/PEP. (a) bare GCE (b) GCE/PEDOT/PEP (c) GCE/PEDOT/PEP/C1 (d) GCE/PEDOT/PEP/C1/MB (e) GCE/PEDOT/PEP/C1/MB/T2 (f) the electrochemical response change of (d) and (e).

was then carried out by dipping GCE/PEDOT/PEP/C1/MB into PBS (0.2 M, pH 7.4) containing different concentration of target DNA (T2) for 90 min at room temperature. The electrodes obtained from this process were denoted as GCE/PEDOT/PEP/C1/MB/T2. The differential pulse voltammetry (DPV) signals for MB (using GCE/PEDOT/PEP/C1/MB and GCE/PEDOT/PEP/C1/MB/T2) were measured in blank PBS (0.2 M, pH 7.4). The DPV parameters are as follows: potential range, from −0.35 to 0.21 V; potential increment, 4 mV; amplitude, 50 mV; pulse period, 0.5 s. The MB electrochemical signal of GCE/PEDOT/PEP/C1/MB was considered the background. To test the specificity of the assay, different DNA sequences (M1, M2 and M3) were utilized as controls.

2.5. Characterization of antifouling ability

5% (V/V) human plasma, 2% (V/V) human serum and four single protein solutions (1.0 ng mL^{-1}) were prepared in advance for use in the antifouling experiments. DPV technique was employed to monitor protein adsorption on the surfaces of PEDOT/PEP and PEDOT/$LiClO_4$. The DPV measurements were performed in 0.2 M PBS (pH 7.4) containing 5.0 mM $[Fe(CN)_6]^{3-/4-}$ and 0.1 M KCl. The DPV parameters were as follows: potential increment of 4.0 mV; amplitude of 50 mV; and pulse period of 0.5 s. The DPV responses of PEDOT/PEP and PEDOT/$LiClO_4$ surfaces before and after incubation (incubated with single protein solution or complex media for 30 min, followed by washing with PBS and water) were recorded, and the changes were compared.

3. Results and discussion

3.1. Characteristics of the modified electrodes.

Morphology and microstructure have a significant impact on the performance of conducting polymers [39]. The surface morphologies and microstructures of the PEDOT/$LiClO_4$ and PEDOT/PEP films were characterized by SEM with an acceleration voltage of 5.0 kV. PEDOT/$LiClO_4$ and PEDOT/PEP nanocomposites have very distinct morphologies. Fig. 1A and B show that the PEDOT/$LiClO_4$ composite is relatively flat with only slight roughness. Interestingly the PEDOT/PEP nanocomposite has a highly porous network morphology (Fig. 1C and D). PEDOT can be polymerized by chemical or electrochemical oxidation methods from 3,4-ethylenedioxythiophene (EDOT) monomers. During polymerization, the positively charged PEDOT backbones need to be neutralized by negatively charged ions from various chemicals, such as graphene oxide (GO) [40], 4-arm poly(ethylene glycol) (PEG) terminated with thiol groups [41] , poly(styrene sulfonic acid) [42], ionic liquids (ILs) [43] and so on. Since the synthesized polypeptide possesses carboxylic groups and thiol groups that are negatively charged in neutral solution, the polypeptide may be incorporated into PEDOT through polymerization. The formation of such a 3D porous structure may be due to the doping of the polypeptide into the conducting polymer, which can act as a "soft template" for the growth of the conducting polymer PEDOT. The dopant can guide the morphology of the conducting polymer composite, and this mechanism has been confirmed in previous studies [44]. It is clear that the PEDOT/PEP nanocomposite has a large specific area for aptamer immobilization.

To build an antifouling interface, a super hydrophilic interface is highly desired, which markedly contributes to resisting nonspecific protein adsorption [45,46]. To assess the hydrophilicity of the modified interfaces, the static water contact angles of bare ITO, ITO/PEDOT/$LiClO_4$ and ITO/PEDOT/PEP were tested (Fig. 2 and Table S2). The bare ITO had a contact angle of 63.77°. The contact angle decreased to 27.33° after the modification with PEDOT/$LiClO_4$, exhibiting that the synthetic PEDOT film is moderately hydrophilic. More interestingly, for the PEDOT/PEP modified surface, an even smaller contact angle of 8.99° was obtained, demon-

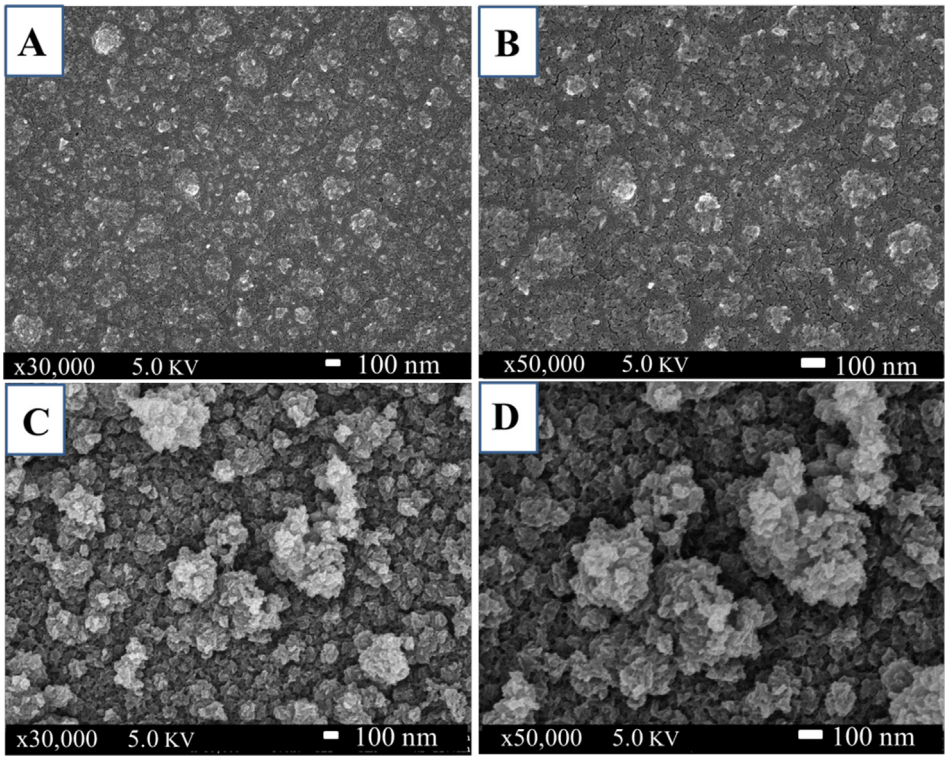

Fig. 1. SEM images of (A, B) PEDOT/$LiClO_4$ films and (C, D) PEDOT/PEP films. A and C (x30,000), B and D (x50,000), respectively, are the same magnification.

strating the high hydrophilicity of the composite. The contact angle of PEDOT/PEP is much smaller than that of other antifouling surfaces, such as polyethylene glycol modified surface (22.4°) [38] and hyaluronic acid doped PEDOT composite (19.0°) [47]. This may be due to the significant roughness of the surface and the fact that the polypeptides contain a large number of amino and carboxyl groups that are easily hydrated.

The XPS spectra also demonstrated the successful preparation of the PEDOT/$LiClO_4$ and PEDOT/PEP nanomaterials and the fixation of the DNA probes. In the XPS analysis, PEDOT/$LiClO_4$ showed C 1 s, O 1 s, and S 1 s peaks, which corresponded to PEDOT (Fig. 3A). Compared to those of PEDOT/$LiClO_4$, PEDOT/PEP showed C 1 s, O 1 s, S 1 s and N 1 s peaks, of which the new N 1 s peak was derived from the dopant polypeptide. The XPS results confirmed that the two conducting polymer nanocomposites were successful prepared. Subsequently, after the DNA probes were attached onto the PEDOT/PEP nanocomposites, the C 1 s and S 1 s peaks decreased, along with the appearance of a new P 2p peak, suggesting the successful attachment of the DNA probes. Quantitative analysis of the surface components of ITO/PEDOT/$LiClO_4$, ITO/PEDOT/PEP and ITO/PEDOT/PEP/C1 are shown in Table S3.

3.2. The antifouling performance of PEDOT/PEP and PEDOT/$LiClO_4$

To evaluate the antifouling ability of the composites, the DPV response changes of PEDOT/PEP and PEDOT/$LiClO_4$ surfaces were recorded after incubation in four single protein solutions (concentration of 1.0 ng mL^{-1}) or complex media (human saliva and human serum samples) for 30 min at room temperature. The DPV measurements were performed in 0.2 M PBS (pH 7.4) containing 5.0 mM $[Fe(CN)_6]^{3-/4-}$ and 0.1 M KCl. As shown in Fig. 4 (A and B), the PEDOT/PEP surface exhibited a significantly smaller rate of change for the DPV peak current compared with the PEDOT/$LiClO_4$ surface, whether after incubating in the protein solutions or the complex media. As shown in Fig. 4B, for the PEDOT/PEP surface after incubation in 5% human plasma and 2% human serum, the $\Delta i_p/i_0$ changed by 8.12% and 7.12%, respectively, proving the good antifouling ability of the interface containing polypeptides in the natural complex media [19].

3.3. Electrochemical characterization of the biosensor

Cyclic voltammetry (CV) is a valuable and facile technique to characterize the step-by-step construction procedure of the modified electrodes. Characteristic CV plots of various electrodes in two electrochemical probe solutions are shown in Fig. 5 and Fig S1. The bare GCE showed a pair of well-defined redox peaks in PBS (10 mM, pH 7.4) containing 5.0 mM $[Fe(CN)_6]^{3-/4-}$ and 0.1 M KCl (Fig. 5, figure a). A large increase in the peak current was observed when PEDOT/PEP was deposited onto the GCE (figure c), which is slightly larger than the peak current than that of PEDOT/$LiClO_4$ (figure b). This is caused by PEDOT/PEP having larger specific surface area, which demonstrates the good electron transfer property of modified electrode. Predictably, there was a slight decline in the peak currents after the DNA probes were further attached onto the PEDOT/PEP modified electrode. The negatively charged phosphoric acid backbones of the DNA probes repelled the negative $[Fe(CN)_6]^{3-/4-}$ probe and restricted the electron movement (curve c) [48]. Tests in the $[Ru(NH_3)_6]^{2+/3+}$ solution after the immobilization of the DNA probes, the oxidation show that peak current significantly increased and the peak potential shifted to the left (Fig. S2), indicating that the DNA probes facilitate the exchange of electrons at the electrode surface. This is because the negatively charged phosphate backbones of DNA probes attract the positively charged $[Ru(NH_3)_6]^{2+/3+}$ probe and accelerated the electron transfer rate of the $[Ru(NH_3)_6]^{2+/3+}$ probe. Therefore, these results verified that the DNA biosensor functioned as proposed in Scheme 1.

3.4. DNA sensing by the indicator MB

A redox indicator of MB was used to enhance the sensing signal in the detection of BRCA1 using the DPV signal changes produced

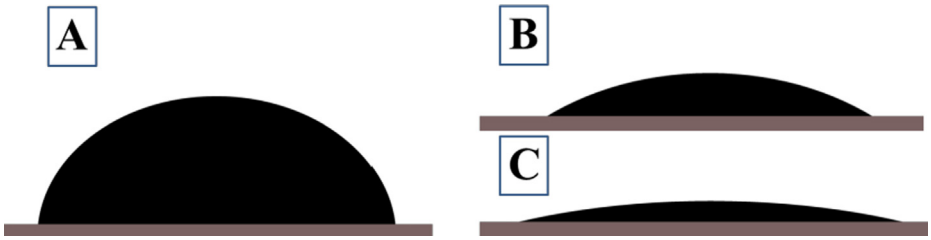

Fig. 2. Graphical representations of contact angles for (A) bare ITO (63.77°), (B) ITO/PEDOT/$LiClO_4$ (27.33°) and (C) ITO/PEDOT/PEP (8.99°) surfaces.

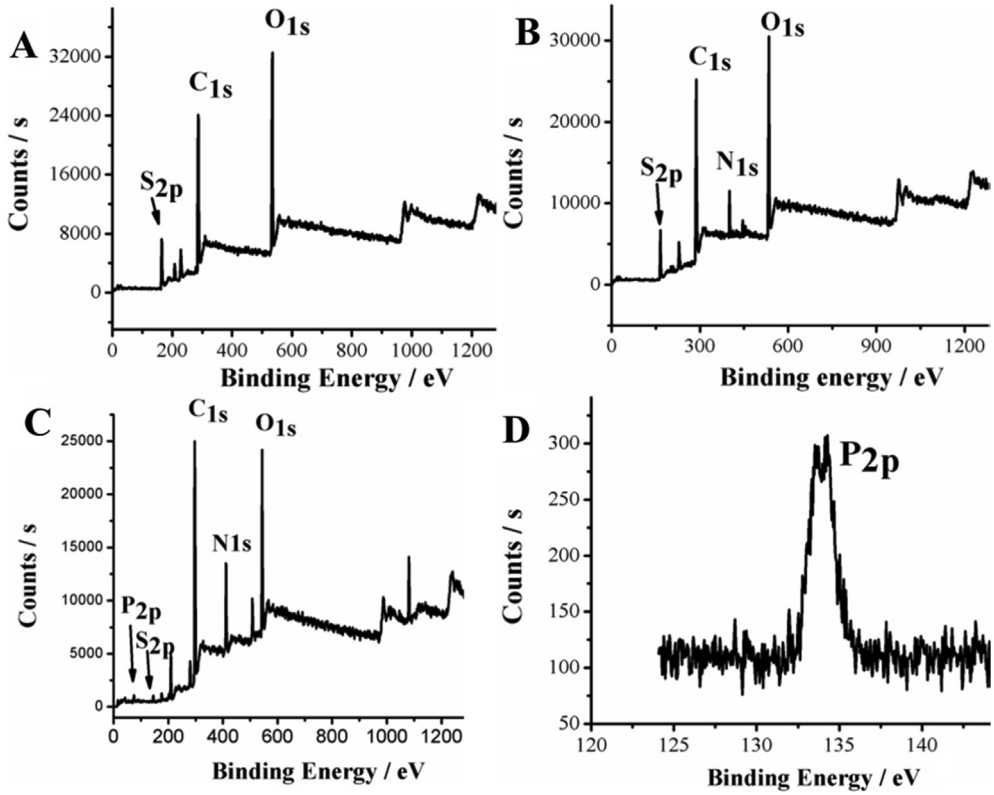

Fig. 3. X-ray photoelectron spectra (XPS) of (A) ITO/PEDOT/$LiClO_4$ (B) ITO/PEDOT/PEP and (C) ITO/PEDOT/PEP/C1. Figure D is an enlarged version of P2p, which are originated from (C) ITO/PEDOT/PEP/C1.

by the hybridization reaction between the capture probes (C1) and the target BRCA1 (T2). The peak current of GCE/PEDOT/PEP/C1/MB was considered the original signal (i_0) and the change rate of MB ($\Delta i_p/i_0$) after BRCA1 hybridization had a corresponding relationship with the BRCA1 concentration under the optimal conditions. GCE/PEDOT/PEP/C1 displayed a straight line with no apparent signal (Fig. 6, curve a). Both GCE/PEDOT/PEP/C1/MB (curve b) and GCE/PEDOT/PEP/C1/MB/T2 (curve c) showed well DPV responses at approximately −0.109 V, which are due to the electrochemical reduction of MB [37]. At the same time, the DPV peak of GCE/PEDOT/PEP/C1/MB/T2 decreased significantly compared with that of GCE/PEDOT/PEP/C1/MB. MB molecules were bound to the single-stranded DNA (ssDNA) through electrostatic interaction between the negatively charged DNA phosphate groups and MB, and specifically, the interactions between the DNA guanine bases and MB [49]. When the target BRCA1 was specifically bound to the attached DNA capture probes, the MB molecules would be dissociated from the ssDNA, resulting in a clear decrease of the MB reduction current. Based on the change of the MB peak current, BRCA1 could be detected sensitively and selectively.

We optimized the following experimental conditions, as shown in Fig. S3 A-D. The concentration of MB was selected as 20 μM. The attachment time for C1 was optimized to 120 min. The MB combination time onto C1 was chosen to be 60 min and the C1-T2 hybridization reaction time was selected as 90 min.

3.5. Analytical performances of the DNA sensors

Fig. 7 shows that well-defined DPV responses are observed at a series of the BRCA1 concentrations under the optimal experimental conditions and the peak current decreased with increased BRCA1 concentrations. The peak current change rate ($\Delta i_p/i_0$) had a good linear relationship with the logarithm of the BRCA1 concentrations within the range from 0.01 pM to 1 nM. The corresponding regression equation can be expressed by $\Delta i_p/i_0 = 1.0921 + 0.0686 \log C$ ($R^2 = 0.994$), with a limit of detection (LOD) of 0.0034 pM (S/N = 3). The LOD is larger than that reported by Zhang's group [50], equivalent to that reported by Luo's group [33], and much smaller than many previous reported values [51,52], as summarized in Table S4. The performance of the fabricated biosensor is

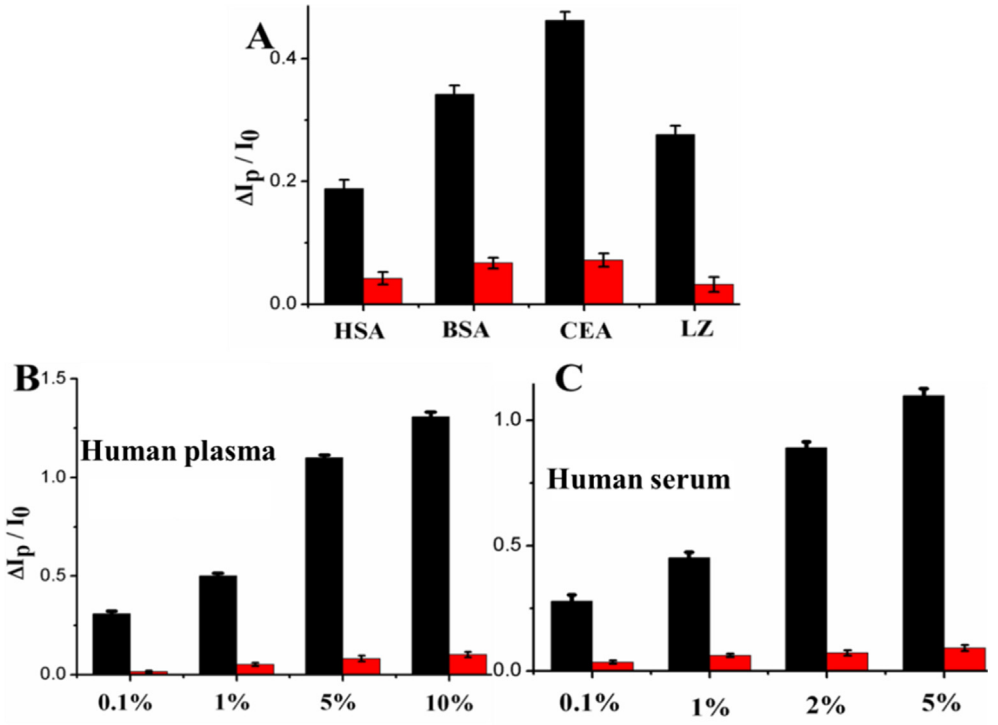

Fig. 4. (A) The DPV current change of GCE/PEDOT/$LiClO_4$ (black rectangles) and GCE/PEDOT/PEP (red rectangles) after incubation in single protein solution. (B) The DPV current change of GCE/PEDOT/$LiClO_4$ (black rectangles) and GCE/PEDOT/PEP (red rectangles) after incubation in complex media. Human plasma and human serum were diluted (V/V) with PBS (pH 7.4, 10 mM,) including NaCl (150 mM). (For interpretation of the references to colour in this figure legend, the reader is referred to the web version of this article.)

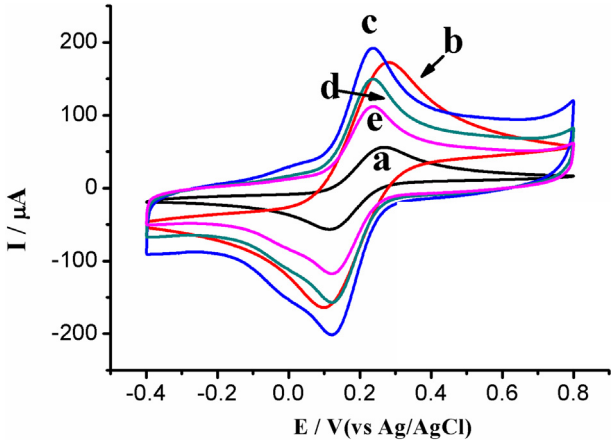

Fig. 5. CV measurements of different modified electrodes in $[Fe(CN)6]^{3-/4-}$ solution. Figures a, b, c, d and e represent bare GCE, PEDOT/$LiClO_4$, PEDOT/PEP, PEDOT/PEP/C1 and PEDOT/PEP/C1/T2 modified GCE, respectively.

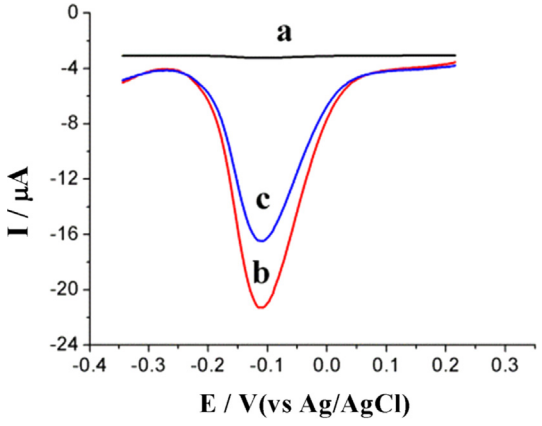

Fig. 6. DPV curves of GCE/PEDOT/PEP/C1 (curve a), GCE/PEDOT/PEP/C1/MB (curve b) and GCE/PEDOT/PEP/C1/MB/T2 (curve c) in PBS (0.2 M, pH = 7.4). T2 concentration is 1.0×10^{-11} M.

satisfactory, which is mainly attributed to the following reasons. (i) The 3D porous nanostructures of PEDOT/PEP can provide more available active sites for the capture DNA binding and improve the electrochemical properties of the transducer. (ii) The biocompatibility of the prepared hydrophilic PEDOT/PEP nanocomposite is beneficial for the capture DNA to maintain biological activity and provide a strong binding force for the target BRCA1.

3.6. Specificity, reproducibility and reusability properties of the biosensor

To estimate reproducibility of the DNA biosensor, six independent biosensors were constructed for the detection of 1.0 pM BRCA1 (Fig. S4A), and the relative standard deviation (RSD) was 3.50%. At the same time, a single biosensor was utilized to assay 1.0 pM BRCA1 six times, and the RSD was 2.31% (Fig. S4B). These results show the satisfactory precision and reproducibility of the biosensor.

To assess the selectivity of the biosensor towards BRCA1, the DPV response change rate ($\Delta i_p/i_0$) of the biosensor was measured in 1.0 pM BRCA1, 1.0 pM mismatched DNA (M1, M2 and M3) and 1.0 ng L^{-1} of different interfering substances (HSA, AFP and LZ). HSA (pI = 4.7–4.9) and LZ (pI = 11.0–11.2) have different isoelectric point (pI). These proteins are either positively or negatively charged in PBS (pH 7.4). AFP is a disease marker in serum. Therefore, HSA, AFP and LZ have been selected as representative interference substances. As shown in Fig. S5, the biosensor showed

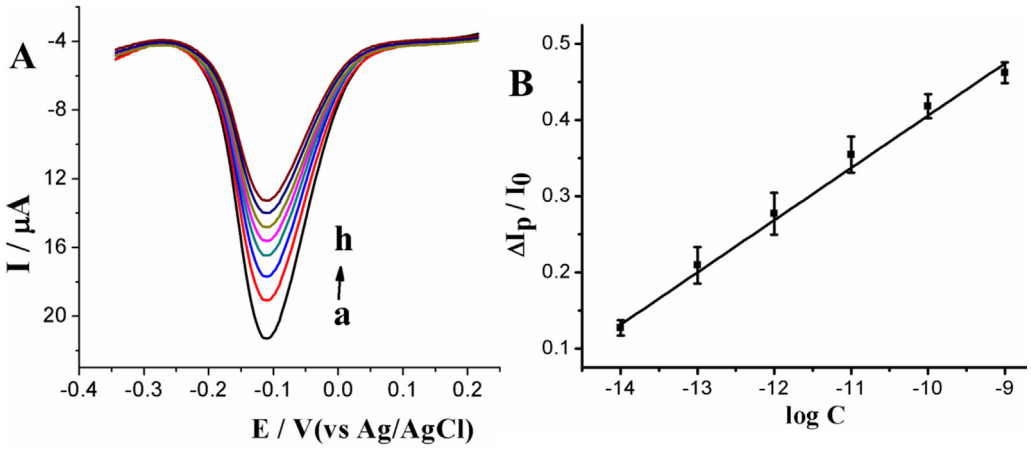

Fig. 7. (A) DPV responses of the biosensor towards different concentrations of target BRCA1 and (B) the calibration curve of the biosensor as a function of BRCA1 concentrations in PBS (0.2 M, pH 7.4). Inset shows the corresponding calibration curve. Fig. A, curve a represents the blank solution and curves b – j refers to BRCA1 at the concentrations from 10^{-14} to 10^{-8} mol L^{-1}. Error bars represent the standard deviations of the current change obtained from three repeated determinations.

negligible signal responses to these possible interference species and had great response rate for BRCA1, demonstrating the satisfactory selectivity of the prepared biosensor for the determination of BRCA1.

To assess the reusability of the DNA biosensor, regeneration studies were performed. The biosensor incubated with 1.0 pM BRCA1was treated with 7.0 M urea for 4 min (to disassociate dsDNA) followed by thorough washing with PBS (pH 7.4) and water. As shown in Fig. S6, the response of the biosensor behaved stably after four duplicated measurements.

3.7. Real sample detection

To estimate the practical application of the developed DNA biosensor, quantitative analysis of a series of BRCA1 samples in human blood was performed with the biosensor and the results are summarized in Table S5. Different concentrations of BRCA1 were specifically added into 1% (V/V) human serum samples. The recovery rates were between 95.2% and 105.0%, with RSDs from 3.93% to 5.37%. The PEDOT/PEP-based biosensor has great potential application for real sample analysis.

4. Conclusion

Novel PEDOT/PEP nanocomposites with 3D porous morphology, good biocompatible and excellent hydrophilicity were successfully prepared by electrochemical polymerization. By using the prepared PEDOT/PEP nanocomposites, a sensitive and low fouling DNA biosensor was constructed through the immobilization of capture DNA. Owing to the good conductivity, excellent hydrophilicity and antifouling property of the PEDOT/PEP composite, the immobilized capture DNA retains its high binding affinity, and the biosensor showed satisfactory analytical performance including a low detection limit, high sensitivity and favorable selectivity. Furthermore, the DNA biosensor can directly assay BRCA1 in 1% human serum with negligible effects from protein adsorption. It is expected that PEDOT/PEP nanocomposites can be utilized for the development of antifouling sensors and biosensors.

Declaration of Competing Interest

The authors declare that they have no known competing financial interests or personal relationships that could have appeared to influence the work reported in this paper.

Acknowledgments

This research was supported by the National Natural Science Foundation of China (21705088), Shandong Key Laboratory of Biochemical Analysis (SKLBA2008), Shandong Province Agricultural Application Technology Innovation Project (SD2019NJ001-2), and the Qingdao Agricultural University High-level Talent Project (663/1117025).

Note: All human serum (or plasma) experiments were conducted according to the ethical guidelines of Qingdao Agricultural University and the "3R" principle. All experiments and the research project hereby are approved by the Ethics Committee of Qingdao Agricultural University.

Appendix A. Supplementary material

Supplementary data to this article can be found online at https://doi.org/10.1016/j.bioelechem.2020.107595.

References

[1] I.E. Tothill, Biosensors for cancer markers diagnosis, Semin. Cell Dev. Biol. 20 (2009) 55–62.
[2] M. Lv, Y. Liu, J. Geng, X. Kou, Z. Xin, D. Yang, Engineering nanomaterials-based biosensors for food safety detection, Biosens. Bioelectron. 106 (2018) 122–128.
[3] C.S. Pundir, N. Yadav, A.K. Chhillar, Occurrence, synthesis, toxicity and detection methods for acrylamide determination in processed foods with special reference to biosensors: A review, Trends Food. Sci. Technol. (2019).
[4] R. Gui, H. Jin, H. Guo, Z. Wang, Recent advances and future prospects in molecularly imprinted polymers-based electrochemical biosensors, Biosens. Bioelectron. 100 (2018) 56–70.
[5] H.L. El, I. Bourais, H. Mohammadi, A. Amine, Recent Advances in Electrochemical Biosensors Based on Enzyme Inhibition for Clinical and Pharmaceutical Applications, Sensors 18 (2018) 164.
[6] I. Banerjee, R.C. Pangule, R.S. Kane, Antifouling Coatings: Recent Developments in the Design of Surfaces That Prevent Fouling by Proteins, Bacteria, and Marine Organisms, Adv. Mater. 23 (2011) 690–718.
[7] H. Vaisocherová, E. Brynda, J. Homola, Functionalizable low-fouling coatings for label-free biosensing in complex biological media: advances and applications, Analy. Bioanaly. Chem. 407 (2015) 3927–3953.
[8] C. Blaszykowski, S. Sheikh, M. Thompson, A survey of state-of-the-art surface chemistries to minimize fouling from human and animal biofluids, Biomater. Sci. 3 (2015) 1335–1370.
[9] K.L. Prime, G.M. Whitesides, Self-assembled organic monolayers: model systems for studying adsorption of proteins at surfaces, Science 252 (1991) 1164–1167.
[10] B.R. Knowles, P. Wagner, S. Maclaughlin, M.J. Higgins, P.J. Molino, Silica nanoparticles functionalized with zwitterionic sulfobetaine siloxane for application as a versatile antifouling coating system, Acs Appl. Mater. Interfaces 9 (2017) 18584–18594.

[11] D. Hong, H.C. Hung, K. Wu, X. Lin, F. Sun, P. Zhang, S. Liu, K.E. Cook, S. Jiang, Achieving Ultralow Fouling under Ambient Conditions via Surface-Initiated ARGET ATRP of Carboxybetaine, Acs Appl. Mater. Interf. 9 (2017) 9255–9259.
[12] J.O. Zoppe, N.C. Ataman, P. Mocny, J. Wang, J. Moraes, H.A. Klok, Surface-Initiated Controlled Radical Polymerization: State-of-the-Art, Opportunities, and Challenges in Surface and Interface Engineering with Polymer Brushes, Chem. Rev. 117 (2017) 1105–1318.
[13] C. Shengfu, Z. Jie, L. Lingyan, J. Shaoyi, Strong resistance of phosphorylcholine self-assembled monolayers to protein adsorption: insights into nonfouling properties of zwitterionic materials, J. Am. Chem. Soc. 127 (2005) 14473.
[14] Y.S. Gao, J.K. Xu, L.M. Lu, X.F. Zhu, W.M. Wang, T.T. Yang, K.X. Zhang, Y.F. Yu, A label-free electrochemical immunosensor for carcinoembryonic antigen detection on a graphene platform doped with poly (3, 4-ethylenedioxythiophene)/Au nanoparticles, RSC Adv. 5 (2015) 86910–86918.
[15] Z. Zheng, C. Shengfu, J. Shaoyi, Dual-functional biomimetic materials: nonfouling poly(carboxybetaine) with active functional groups for protein immobilization, Biomacromolecules 7 (2006) 3311–3315.
[16] G. Cheng, H. Xue, Z. Zhang, S. Chen, S. Jiang, A Switchable Biocompatible Polymer Surface with Self-Sterilizing and Nonfouling Capabilities, Angew. Chem. Int. Ed. 47 (2008) 8831–8834.
[17] H. Ye, L. Wang, R. Huang, R. Su, B. Liu, W. Qi, Z. He, Superior antifouling performance of a zwitterionic peptide compared to an amphiphilic, non-ionic peptide, Acs Appl. Mater. Interf. 7 (2015) 22448–22457.
[18] H. Wang, F. Cheng, W. Shen, G. Cheng, J. Zhao, W. Peng, J. Qu, Amino acid-based anti-fouling functionalization of silica nanoparticles using divinyl sulfone, Acta Biomater. 40 (2016) 273–281.
[19] A.K. Nowinski, F. Sun, A.D. White, A.J. Keefe, S. Jiang, Sequence, structure, and function of peptide self-assembled monolayers, J. Am. Chem. Soc. 134 (2012) 6000–6005.
[20] R. Chelmowski, S.D. Köster, A. Kerstan, A. Prekelt, C. Grunwald, T. Winkler, N. Metzler-Nolte, A. Terfort, C. Wöll, Peptide-based SAMs that resist the adsorption of proteins, J. Am. Chem. Soc. 130 (2008) 14952–14953.
[21] M.R. Abidian, K.A. Ludwig, T.C. Marzullo, D.C. Martin, D.R. Kipke, Interfacing conducting polymer nanotubes with the central nervous system: chronic neural recording using poly (3, 4-ethylenedioxythiophene) nanotubes, Adv. Mater. 21 (2009) 3764–3770.
[22] X. Wang, P. Sjöberg-Eerola, J.-E. Eriksson, J. Bobacka, M. Bergelin, The effect of counter ions and substrate material on the growth and morphology of poly (3, 4-ethylenedioxythiophene) films: Towards the application of enzyme electrode construction in biofuel cells, Synth. Met. 160 (2010) 1373–1381.
[23] J. Bobacka, A. Lewenstam, A. Ivaska, Electrochemical impedance spectroscopy of oxidized poly (3, 4-ethylenedioxythiophene) film electrodes in aqueous solutions, J. Electroanal. Chem. 489 (2000) 17–27.
[24] E. Poverenov, M. Li, A. Bitler, M. Bendikov, Major effect of electropolymerization solvent on morphology and electrochromic properties of PEDOT films, Chem. Mater. 22 (2010) 4019–4025.
[25] C.K. Nash, I. Fritsch, Poly (3, 4-ethylenedioxythiophene)-modified electrodes for microfluidics pumping with redox-magnetohydrodynamics: improving compatibility for broader applications by eliminating addition of redox species to solution, Anal. Chem. 88 (2016) 1601–1609.
[26] S.C. Luo, E. Mohamed Ali, N.C. Tansil, H.-H. Yu, S. Gao, E.A. Kantchev, J.Y. Ying, Poly (3, 4-ethylenedioxythiophene)(PEDOT) nanobiointerfaces: thin, ultrasmooth, and functionalized PEDOT films with in vitro and in vivo biocompatibility, Langmuir 24 (2008) 8071–8077.
[27] S.M. Richardson-Burns, J.L. Hendricks, B. Foster, L.K. Povlich, D.-H. Kim, D.C. Martin, Polymerization of the conducting polymer poly (3, 4-ethylenedioxythiophene)(PEDOT) around living neural cells, Biomaterials 28 (2007) 1539–1552.
[28] J. Qiu, X. Kang, L. Ma, W. Huang, Q. Ge, Preparation and application of poly 3, 4-ethylenedioxythiophene (PEDOT) nanofibers in the pretreatment of samples before the determination of elements in children fingernails, in: IOP Conference Series: Materials Science and Engineering, IOP Publishing, 2015, p. 012093.
[29] G. Chao, X.J. Huang, Voltammetric determination of mercury(II), Trends Anal. Chem. 51 (2013) 1–12.
[30] K. Kiilerich-Pedersen, J. Daprà, S. Cherré, N. Rozlosnik, High sensitivity point-of-care device for direct virus diagnostics, Biosens. Bioelectron. 49 (2013) 374–379.
[31] F. Kuralay, S. Demirci, M. Kiristi, L. Oksuz, A.U. Oksuz, Poly (3, 4-ethylenedioxythiophene) coated chitosan modified disposable electrodes for DNA and DNA–drug interaction sensing, Colloids Surf. B 123 (2014) 825–830.
[32] V. Sethuraman, P. Muthuraja, J.A. Raj, P. Manisankar, A highly sensitive electrochemical biosensor for catechol using conducting polymer reduced graphene oxide–metal oxide enzyme modified electrode, Biosens. Bioelectron. 84 (2016) 112–119.
[33] W. Wang, X. Fan, S. Xu, J.J. Davis, X. Luo, Low fouling label-free DNA sensor based on polyethylene glycols decorated with gold nanoparticles for the detection of breast cancer biomarkers, Biosens. Bioelectron. 71 (2015) 51–56.
[34] M. Wezyk, C. Zekanowski, Role of BRCA1 in Neuronal Death in Alzheimer's Disease, ACS Publications (2018).
[35] X. Luo, A.J. Killard, M.R. Smyth, Nanocomposite and nanoporous polyaniline conducting polymers exhibit enhanced catalysis of nitrite reduction, Chemistry-A European Journal 13 (2007) 2138–2143.
[36] J. Chen, J. Zhang, K. Wang, X. Lin, L. Huang, G. Chen, Electrochemical Biosensor for Detection of BCR/ABL Fusion Gene Using Locked Nucleic Acids on 4-Aminobenzenesulfonic Acid-Modified Glassy Carbon Electrode, Anal. Chem. 80 (2008) 8028–8034.
[37] F. Li, J. Peng, Q. Zheng, X. Guo, H. Tang, S. Yao, Carbon Nanotube-Polyamidoamine Dendrimer Hybrid-Modified Electrodes for Highly Sensitive Electrochemical Detection of MicroRNA24, Anal. Chem. 87 (2015) 4806–4813.
[38] N. Hui, X. Sun, S. Niu, X. Luo, PEGylated polyaniline nanofibers: antifouling and conducting biomaterial for electrochemical DNA sensing, Acs Appl. Mater. Interfaces 9 (2017) 2914–2923.
[39] L. Groenendaal, G. Zotti, P.H. Aubert, S.M. Waybright, J.R. Reynolds, Electrochemistry of poly (3, 4-alkylenedioxythiophene) derivatives, Adv. Mater. 15 (2003) 855–879.
[40] W. Wang, G. Xu, X.T. Cui, G. Sheng, X. Luo, Enhanced catalytic and dopamine sensing properties of electrochemically reduced conducting polymer nanocomposite doped with pure graphene oxide, Biosen. Bioelectron. 58 (2014) 153–156.
[41] M. Cui, Z. Song, Y. Wu, B. Guo, X. Fan, L. Xiliang, A highly sensitive biosensor for tumor maker alpha fetoprotein based on poly(ethylene glycol) doped conducting polymer PEDOT, Biosen. Bioelectron. 79 (2016) 736–741.
[42] Z.T. Zhu, J.T. Mabeck, C. Zhu, N.C. Cady, C.A. Batt, G.G. Malliaras, A simple poly (3,4-ethylene dioxythiophene)/poly(styrene sulfonic acid) transistor for glucose sensing at neutral pH, Chem. Commun. 1556–1557 (2004).
[43] M. Dobbelin, R. Marcilla, C. Pozo-Gonzalo, D. Mecerreyes, Innovative materials and applications based on poly(3,4-ethylenedioxythiophene) and ionic liquids, J. Mater. Chem. 20 (2010) 7613–7622.
[44] Sakmeche N., Aeiyach S., A.J. J., Improvement of the Electrosynthesis and Physicochemical Properties of Poly(3,4-ethylenedioxythiophene) Using a Sodium Dodecyl Sulfate Micellar Aqueous Medium, Langmuir 15 (1999) 2566-2574.
[45] S. Lowe, N.M. OBrien-Simpson, L.A. Connal, Antibiofouling Polymer Interfaces: Poly(ethylene glycol) and Other Promising Candidates, Polym. Chem. 6 (2015) 198–212.
[46] C. Jiang, G. Wang, R. Hein, N. Liu, X. Luo, J.J. Davis, Antifouling Strategies for Selective In Vitro and In Vivo Sensing, Chem. Rev. 120 (2020) 3852–3889.
[47] W. Wang, M. Cui, Z. Song, X. Luo, An antifouling electrochemical immunosensor for carcinoembryonic antigen based on hyaluronic acid doped conducting polymer PEDOT, RSC Adv. 6 (2016) 88411–88416.
[48] L. Wang, E. Hua, M. Liang, C. Ma, Z. Liu, S. Sheng, M. Liu, G. Xie, W. Feng, Graphene sheets, polyaniline and AuNPs based DNA sensor for electrochemical determination of BCR/ABL fusion gene with functional hairpin probe, Biosens. Bioelectron. 51 (2014) 201–207.
[49] R. Gangopadhyay, A.D. Chowdhury, A. De, Functionalized polyaniline nanowires for biosensing, Sens. Actuat. B 171 (2012) 777–785.
[50] X. Qin, S. Xu, L. Deng, R. Huang, X. Zhang, Photocatalytic electrosensor for label-free and ultrasensitive detection of BRCA1 gene, Biosens. Bioelectron. 85 (2016) 957–963.
[51] X. Ren, T. Yan, S. Zhang, X. Zhang, P. Gao, D. Wu, B. Du, Q. Wei, Ultrasensitive dual amplification sandwich immunosensor for breast cancer susceptibility gene based on sheet materials, Analyst 139 (2014) 3061–3068.
[52] S. Shimron, F. Wang, R. Orbach, I. Willner, Amplified detection of DNA through the enzyme-free autonomous assembly of hemin/G-quadruplex DNAzyme nanowires, Analy. Chem. 84 (2011) 1042–1048.